Biodiversity monitoring in urban community gardens using proximal sensing and drone remote sensing

Afrasiabian, Y.; Contiz, F.; Cleemput, E.E.A. van; Egerer, M.; Yu, K.

Remote Sensing Applications: Society and Environment 39 (2025) 101685

Contents lists available at ScienceDirect

Remote Sensing Applications: Society and Environment

journal homepage: www.elsevier.com/locate/rsase

Biodiversity monitoring in urban community gardens using proximal sensing and drone remote sensing

Yasamin Afrasiabian [a], Felix Contiz [b], Elisa Van Cleemput [c], Monika Egerer [b], Kang Yu [a,*]

[a] Precision Agriculture Lab, TUM School of Life Sciences, Technical University of Munich, Dürnast 9, 85354, Freising, Germany
[b] Urban Productive Ecosystems, TUM School of Life Sciences, Technical University of Munich, Hans Carl-von-Carlowitz-Platz 2, 85354, Freising, Germany
[c] Leiden University College the Hague, Leiden University, Anna van Buerenplein 301, 2595 DG, Den Haag, the Netherlands

ARTICLE INFO

Keywords:
Biodiversity conservation
Drone remote sensing
Field spectroscopy
Urban green
Spectral diversity hypothesis
Height variation hypothesis

ABSTRACT

In urban community gardens, artificially managed ground cover types, including vegetative and non-vegetative ground components, are both critical to ecological functioning. Yet, how these non-vegetative components influence spectral diversity in ways that are different from natural systems has not been addressed. This study investigated the potential of combining spectral and structural diversity variables, corresponding to the Spectral Variation and Height Variation Hypotheses, respectively, to monitor plant and ground cover diversity. These variables were derived from in situ hyperspectral measurements, drone-based multispectral imagery, and three-dimensional canopy height models. We examined four biodiversity variables, including plant species richness, total plant abundances, ground cover entropy, and ground cover richness, across five urban community gardens over two years. Spectral diversity was calculated based on the Coefficient of Variation (CV), Spectral Angle Mapper (SAM), and Shannon's Entropy (Entropy) indices at multiple spectral ranges. Structural diversity variables, including canopy height variation and image texture features. Our results showed that Red-Edge and Near-infrared (NIR) bands effectively captured compositional variation in ground cover, while visible wavelengths better reflected subtle differences in vegetative components. Texture features and height-based structural variables provided valuable insights into canopy complexity, particularly improving predictions of plant abundance and ground cover entropy. Finally, we found that integrating spectral and structural diversity variables further enhanced predictive performance due to considering canopy biochemical and structural differences. This multi-metric approach outperformed single-source analyses, underscoring the value of combining complementary remote sensing data for better interpreting urban garden biodiversity. Our findings highlight the importance of characterizing canopy structural heterogeneity in advancing biodiversity monitoring within these complex urban ecosystems.

1. Introduction

Urban community gardens, characterized by heterogeneous three-dimensional structure, have emerged as vital components of

* Corresponding author. TUM Precision Agriculture Lab, Dürnast 9, 85354, Germany.
E-mail address: kang.yu@tum.de (K. Yu).

https://doi.org/10.1016/j.rsase.2025.101685
Received 12 February 2025; Received in revised form 13 June 2025; Accepted 3 August 2025
Available online 7 August 2025

urban ecosystems, substantially contributing to biodiversity conservation and the delivery of essential ecosystem services (Egerer et al., 2017; Lin and Philpott, 2015). These green spaces host a wide range of plant species and ground cover types, including rocks, herbaceous vegetation, bare soil, and mulches. This structural complexity not only influences plant diversity but also creates habitats and nesting sites for various wildlife, including key pollinators like bees, insects, and butterflies (Rocchini et al., 2010a; St-Louis et al., 2006; Tuanmu and Jetz, 2015; Wang and Gamon, 2019). However, while this high heterogeneity enhances ecological resilience, it poses challenges for traditional field-based biodiversity assessments, which are often labor-intensive, time-consuming, and may not adequately capture fine-scale spatial variability (Fj Aronson et al., 2017; Turner et al., 2003). Although remote sensing technologies offer promising alternatives, they have mainly been applied more commonly in natural ecosystems like forests and grasslands (Muro et al., 2022; Rocchini et al., 2010b). Therefore, combining field survey methods and sensing technologies is essential for developing a comprehensive monitoring approach to urban garden heterogeneity and its ecosystem services (Wagner and Egerer, 2022).

Spectral diversity is one of the effective approaches for assessing biodiversity using remotely sensed data. The spectral diversity-biodiversity relationship can be explained by the Spectral Variation Hypothesis (SVH) (Palmer et al., 2002). This hypothesis proposes that increasing variation in the spectral characteristics of an area is positively related to biodiversity (e.g., species richness), because spectral signatures reflect subtle differences in biochemical, physiological, and structural characteristics among species (Van Cleemput et al., 2023). Though this concept has been widely employed in forestry and grassland for monitoring plant biodiversity and species richness, the results are not necessarily generalizable to other systems, as discrepancies sometimes arise, e.g., some supporting SVH while others report weak or negative relationships (Levin et al., 2007; Rocchini et al., 2010b; White et al., 2010). To our knowledge, testing the SVH in highly heterogeneous urban environments, such as community gardens, remains unexplored. Such environments present substantial challenges due to their complex canopy structures and diverse ground cover types, which complicate the interpretation of spectral diversity and may cause mismatches with survey data. Moreover, spectral diversity assessments in traditional vegetation studies often overlook the non-vegetative ground components, the presence of which can create distinct spectral signatures, further increasing the complexity of understanding the spectral diversity and biodiversity relationship.

Structural diversity concepts, on the other hand, provide critical insights into the three-dimensional arrangement and complexity of canopies, capturing ecosystem heterogeneity that spectral data alone may not fully represent (Anderson et al., 2021; Ishii, 2004). Vegetation structure describes above-ground biomass within an environment, vertically and horizontally (Gadow et al., 2012). Advances in remote sensing technologies, such as Unmanned Aerial Vehicle (UAV)-based RGB point clouds and LiDAR, have facilitated the quantification of structural diversity by generating detailed canopy height models and three-dimensional canopy reconstructions (Torresani et al., 2020; Zhu et al., 2024a). Variations in canopy height play a crucial role in supporting biodiversity by creating a multitude of habitats and niches within an ecosystem (McElhinny et al., 2005). This concept is adapted from the Height Variation Hypothesis (HVH), which posits that ecosystems with increased vertical complexity are more likely to support greater species diversity (Ehbrecht et al., 2017; Torresani et al., 2020). In forest ecosystems, for instance, areas with diverse canopy structures have been shown to support a wider array of plant species due to the range of light conditions, microclimates, and resource availability created by height variations (Schneider et al., 2017). Moreover, image texture analysis across various resolutions has proven effective in capturing the vertical and horizontal patterns of structural and compositional heterogeneity of above-ground diversity (Bellis et al., 2008; Farwell et al., 2021). To date, few studies focus explicitly on structural diversity encompassing non-vegetative ground covers within urban community gardens compared to forests or parks, and remote sensing-based structural diversity assessment in urban community gardens remains limited. Consequently, ground-based and UAV-based measurements of garden canopy structures will improve our understanding of the relationship between biodiversity and spectral diversity.

While both the spectral and structural diversity provide valuable insights into ecosystem heterogeneity, each captures different aspects of biodiversity. Spectral diversity primarily reflects the biochemical and physiological characteristics of vegetation, whereas structural diversity highlights physical organization and three-dimensional variability (Fassnacht et al., 2016). Integrating these metrics has shown the potential to enhance biodiversity assessments by encompassing complementary facets of ecosystem heterogeneity (Asner et al., 2015). However, little is known about which specific spectral and structural diversity variables can effectively characterize biodiversity within highly heterogeneous urban community gardens. Challenges include the fine-scale spatial variability, diverse ground cover types (e.g., bare soil, grass, woodchips), and uneven canopy heights, which lead to overlapping spectral signatures and intricate canopy structures that complicate structural and spectral signal interpretation (Wang et al., 2018).

Urban community gardens exhibit a high ecological heterogeneity, where vegetation grows alongside patches of soil, mulch, and other non-vegetative ground cover at a fine scale. It is unclear whether the spectral diversity-biodiversity relationship still applies, or which spectral and structural information from UAV remote sensing images can explain the spatial heterogeneity. Spectral diversity metrics capture biochemical variation while 3-D structural metrics capture canopy complexity; combining them provides richer biodiversity information for such mixed surfaces. However, the combined use of spectral and structural diversity metrics to study biodiversity in urban community gardens remains underexplored. To address this knowledge gap, this study examines whether integrating spectral and structural diversity variables derived from proximal and remote sensing technologies can enhance the assessment of plant and ground cover diversity in heterogeneous urban community gardens. We hypothesize that the combined use of spectral and structural variables will offer a more accurate and comprehensive understanding of biodiversity patterns, given their specific responses to variations in plant composition, ground cover, and canopy structure. Our specific objectives were to: (1) evaluate the relationship between spectral diversity and biodiversity variables (plant diversity and ground cover diversity), derived from drone multispectral images and proximal hyperspectral data; (2) assess the contribution of image texture features and structural diversity metrics to biodiversity prediction; and (3) determine the effectiveness of integrating both metrics in improving biodiversity assessments.

2. Materials and methods

2.1. Study area and sampling design

The study was conducted in five urban community gardens located in southern Bavaria, within the city of Munich: Essbare Stadt (ESS), Freihamer Freiluftgarten (FF), Karlsfeld Community Garden (KF), StadtAcker (SA), and Sonnengarten Solln (SONN) (Fig. 1). These gardens have been selected to cover varying degrees of urbanization in the Munich area. They vary in geographical locations, elevation, and management practices, as well as in plant and ground cover heterogeneity. Data were collected during 2021 and 2022, with sampling conducted three times per year. Specifically, in 2021, sampling was conducted in July, August, and October, while in 2022, it occurred in May, July, and October (see Fig. 2).

During each sampling round, a 20×20 m plot was generally established in the centre of each garden to standardise the sampling area. Within each selected plot, eight 1×1 m quadrats were randomly placed for data collection (Fig. 1a & b). Therefore, both the plots and quadrats changed in location between rounds and years, and no positions were permanently marked. This approach resulted in 40 random quadrats per round (5 gardens × 8 quadrats), with approximately 120 quadrats per year and a total of 240 quadrats across the study (Table 1). The GPS coordinates of each plot and quadrat were recorded using Real-Time Kinematic (RTK) GPS for precise geolocation.

2.2. Survey data and biodiversity variables

Within each 1 × 1 m^2, we quantified four key biodiversity variables from survey data to test our hypotheses in relation to spectral and structural diversity metrics: (1) plant species richness, defined as the total number of unique plant species per quadrat; (2) total plant abundances, representing the cumulative abundance of all recorded plant species; (3) ground cover richness, calculated as the number of distinct ground cover types present per quadrat; and (4) Ground cover entropy, quantified using Shannon's entropy index (Shannon, 1948) to quantify the heterogeneity of ground cover composition.

Ground cover types were visually estimated in the field based on their proportional coverage, including bare soil, grass, herbaceous vegetation, rock, wood, woodchips, straw, leaf litter, and an "other" category. These categories reflect common substrates in urban

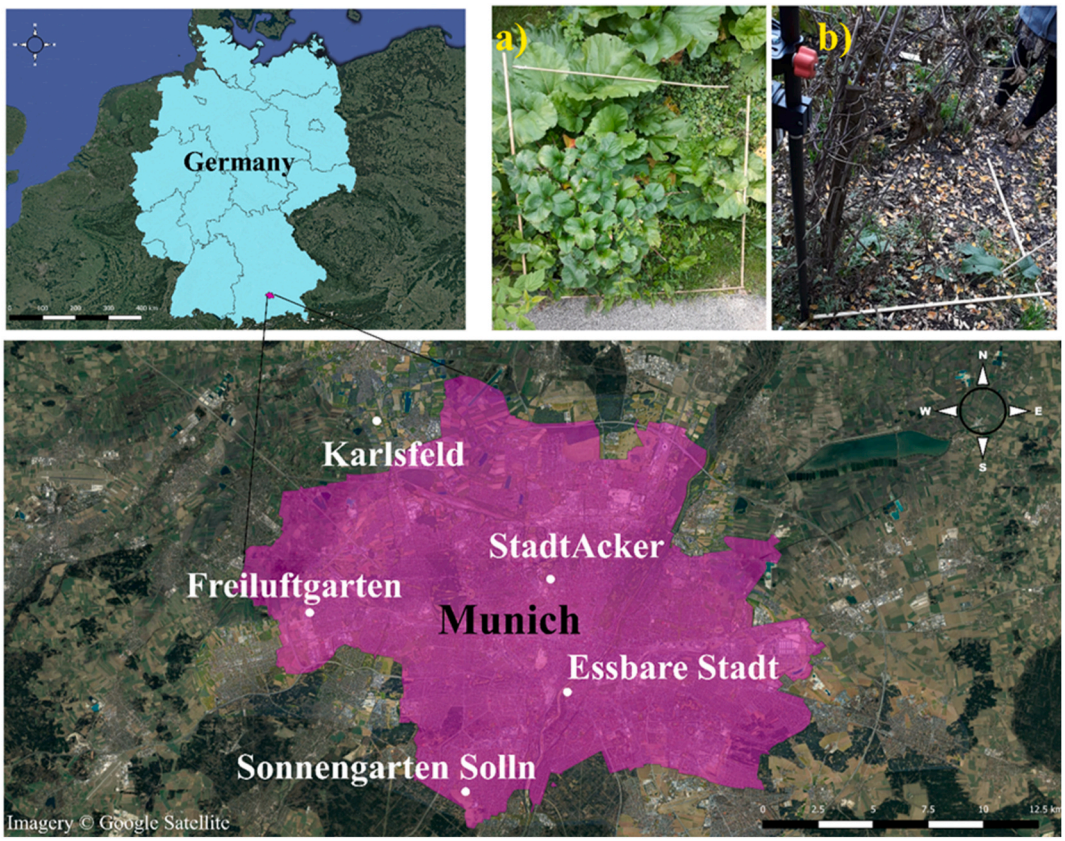

Fig. 1. Location of five community urban gardens in southern Bavaria, Munich, where the data was collected. a) Represents a garden with dense vegetation as indicated by the 1 × 1 m quadrat, indicative of less ground cover diversity, and b) Shows a garden with sparse vegetation and different ground cover types, presenting higher ground cover diversity.

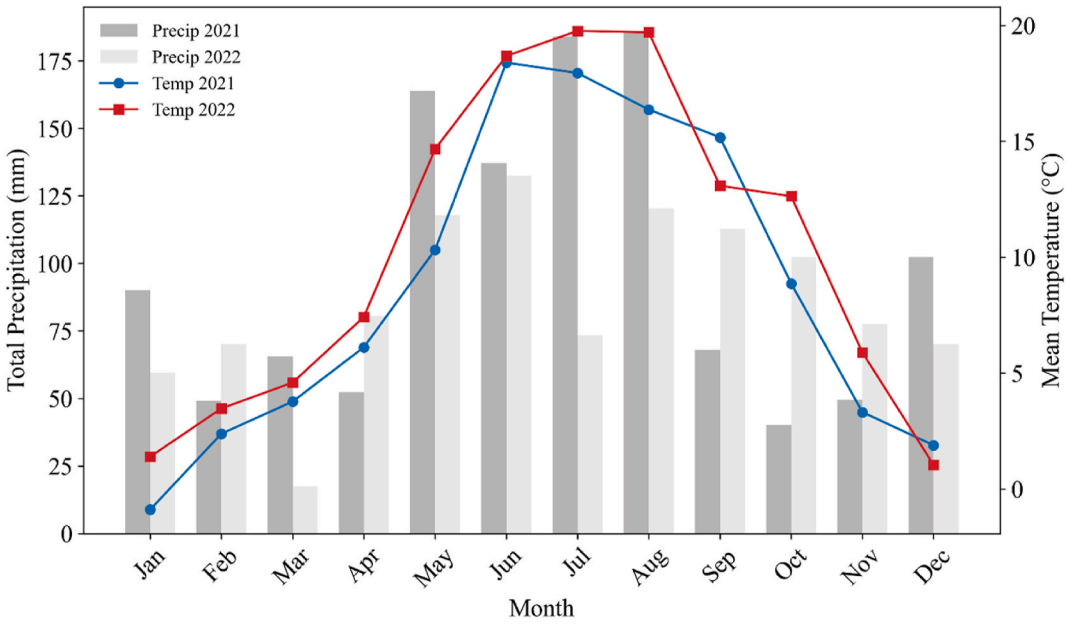

Fig. 2. Monthly precipitation (mm) and air temperature (°C) for Munich in 2021 and 2022, derived from ERA5-Land data.

Table 1
Summary of the five urban community gardens in Munich, including garden area (m^2), mean elevation (m), percentage of built-up area within a 1 km buffer, and the number of 1 × 1 m quadrats sampled in each garden during 2021 and 2022. Garden boundaries were digitized based on UAV-derived data, and built-up area estimates are derived from the ESA WorldCover 10 m land cover product (version 2.0, year 2021).

Garden	Area (m^2)	Mean Elevation (m)	Build-up Area (%)	Quadrats per 2021 (1 × 1 m)	Quadrats per 2022 (1 × 1 m)
ESS	571	563.82	55.31	24	24
FF	756	573.71	33.91	23	24
KF	520	533.14	9.08	24	24
SA	1066	560.28	52.06	23	24
SONN	1210	614.55	26.48	24	24

garden agroecosystems (Lin et al., 2018). Shannon's entropy index was calculated as $-\sum p_i \times ln(p_i)$, where p_i is the relative percent cover of each ground cover type *i*. These four variables indicate plant and ground cover diversity within these urban garden ecosystems.

2.3. Proximal and remotely sensed data acquisition

2.3.1. Proximal ground-based (hyper-) spectroscopic measurements

Proximal hyperspectral measurements (Fig. 3) were acquired using an Analytical Spectral Devices (ASD) spectroradiometer with about 1 nm bandwidths, covering wavelengths from 350 nm to 2500 nm (visible to shortwave infrared) (Analytical Spectral Devices, 1999). Measurements were collected on the exact same day as the ground survey data, between 09:00 and 14:00 under predominantly cloud-free conditions. To minimize the influence of shadowing effects, a single white reference measurement was taken to characterize the incoming irradiance. Subsequently, five randomly selected point measurements were obtained perpendicularly from a height of 1 m to capture the reflected outgoing radiation within each quadrat. In addition, to understand the unique spectral characteristics of individual ground cover types, we conducted five supplementary measurements over homogeneous patches of each identified ground cover category.

Prior to analysis, noisy spectral intervals (350–400 nm and 2400–2500 nm) and strong atmospheric absorption bands (1325–1455 nm and 1775–1970 nm) were excluded. Reflectance values outside the 0–1 range were considered outliers and removed to ensure data quality.

2.3.2. UAV multi-spectral imaging

The Phantom 4 Multispectral RTK (DJI, Shenzhen, China) UAV was used for multispectral image collection (Fig. 3). Multispectral imagery was acquired within 1–3 days of the ground data collection, depending on local weather conditions. The flight altitudes were selected based on the tree heights in the gardens, resulting in varying spatial resolutions: 25 m (13 mm/px for ESS and SA), 20 m (11 mm/px for SONN), and 15 m (8 mm/px for FF and KF). Data processing was performed using Agisoft Metashape 1.8.4 to generate high-

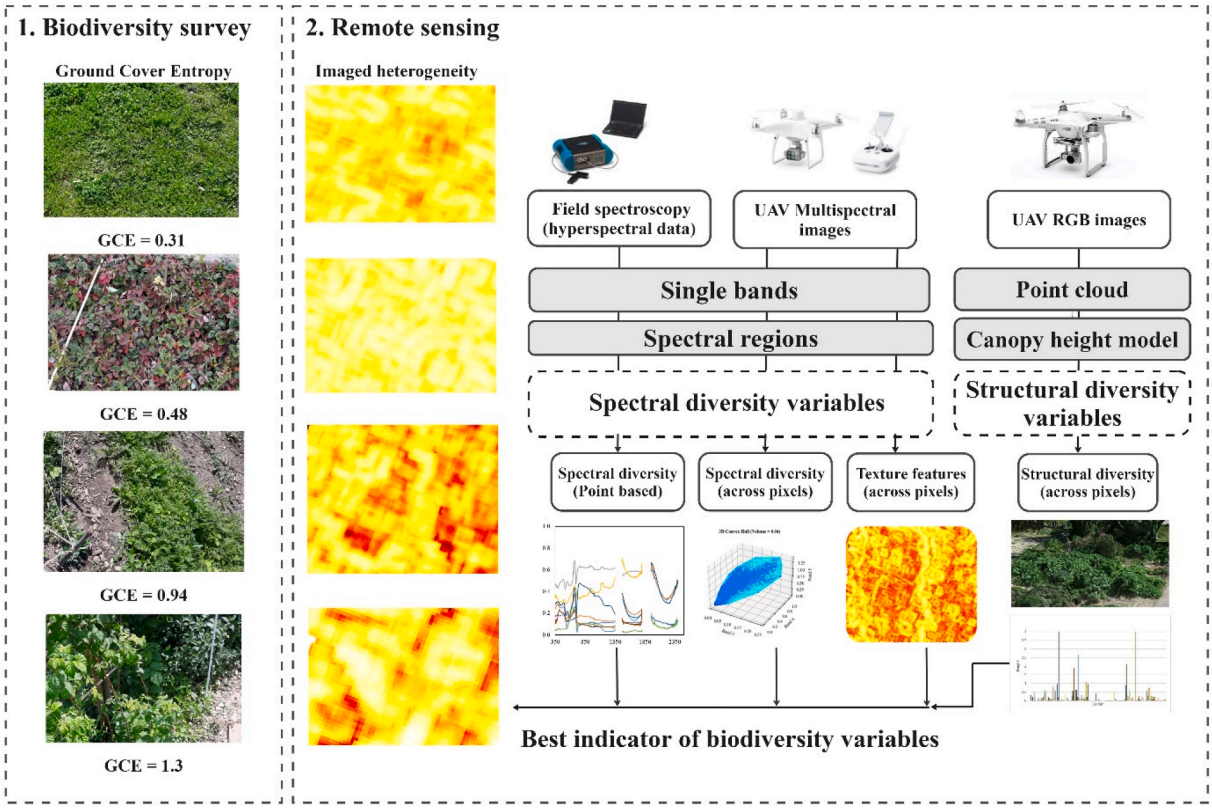

Fig. 3. Flowchart for assessing biodiversity variables using proximal hyperspectral data, UAV multispectral imagery, and RGB point clouds. The workflow begins with ground surveys to document plant species, total abundances, and ground cover types, which are used to calculate ground cover entropy (GCE) and ground cover richness as an indicator of ground cover diversity. Proximal hyperspectral data and UAV multispectral imagery were analyzed to compute spectral diversity variables, considering single spectral bands and different spectral regions, while canopy height models derived from point clouds were used to calculate structural diversity variables. Texture features were also assessed using UAV multispectral imagery.

resolution orthomosaic images. The spectral bands included blue (450 nm ± 16 nm), green (560 nm ± 16 nm), red (650 nm ± 16 nm), red edge (730 nm ± 16 nm), and NIR (840 nm ± 26 nm), with an ISO range from 200 to 800.

2.3.3. UAV RGB-based canopy height

Three-dimensional point clouds were generated from the overlapping RGB images (Fig. 3) captured by the DJI Phantom 4 UAV RTK (DJI, Shenzhen, China) using Agisoft Metashape (version 1.8.4). RGB images were collected on the same day as the UAV multispectral flights. The point clouds were directly produced through photogrammetric processing of the raw RGB imagery. This process involved aligning multiple overlapping images (overlap 90 %) to identify common features and reconstruct the spatial structure, resulting in dense point clouds. These point clouds were subsequently utilized to create Digital Surface Models (DSM) and Digital Terrain Models (DTM), which were then used to derive Canopy Height Models (CHM) by subtracting the DTM from the DSM.

2.4. Proximal and remotely sensed diversity variables

2.4.1. Spectral diversity variables

To evaluate the SVH, we focused on three spectral diversity variables, including the coefficient of variation (CV; e.g. Wang et al., 2016), Shannon's Entropy (Entropy; Shannon, 1948), and Spectral Angle Mapper (SAM; Kruse et al., 1993). These metrics were derived from both field hyperspectral data and the UAV multispectral images (Fig. 3). All variables were calculated for each 1 × 1 m quadrat and then averaged over the wavelength (or band) subsets described below.

2.4.1.1. Band subsets and spectral window. Instead of simulating multispectral bands by applying spectral response functions from the hyperspectral data, we identified wavelength ranges that matched the spectral intervals of our UAV multispectral bands (for example, using the 434–466 nm range in the hyperspectral data to represent the UAV's "blue" band). Within each of these corresponding wavelength ranges (Blue, Green, Red, Red-edge, and NIR), we repeated the CV calculation to ensure that results from the hyperspectral data could be directly compared with those derived from the UAV imagery. We also examined three broader wavelength ranges

including Visible (VIS: 400–700 nm), Red-Edge to Near-Infrared (RE_NIR: 700–1300 nm), and Shortwave Infrared (SWIR: 1500–2400 nm), to see how spectral diversity varied across different parts of the spectrum that relate to biochemical and biophysical of vegetation and ground cover.

2.4.1.2. Proximal spectral diversity variables. Five ASD point spectra were collected per quadrat. For each wavelength λ, we first calculated the mean reflectance (μλ) and its standard deviation (σλ) across the five spectral point measurements (curves). Then, CVλ was calculated using σλ/μλ. CVλ values were finally averaged across all wavelengths (or a specific spectral range, such as NIR) to obtain one CV number per quadrat.

For calculating spectral entropy, each spectrum was converted into a reflectance probability vector by dividing the reflectance at every λ by the spectrum's total reflectance. Spectral entropy was then calculated following - $\sum_{\lambda=1}^{N} p_\lambda \, ln \, p_\lambda$, where p_λ is the reflectance probability and N is the number of valid wavelengths after masking. Quadrat-level entropy is the mean of the five spectrum-level entropies. This "spectral entropy" should not be confused with the ground-cover Shannon index reported in Section 2.2, which is calculated from ground cover survey data, not reflectance.

SAM was obtained by calculating the spectral angle between every pair of the five ASD spectra using $\theta_{i,j} = arccos\left(\frac{R_i . R_j}{\|R_i\| . \|R_j\|}\right)$, where R_i and R_j are the full reflectance vectors (or across a specific spectral window) for measurement *i and j,* and $\|R\|$ is the Euclidean norm (vector length). The mean of all pairwise angles was used as the quadrat-level SAM value. A larger mean SAM indicates greater spectral dissimilarity.

2.4.1.3. Remotely sensed spectral diversity variables. For the UAV imagery, the same operations were performed, but instead of across proximal sensing points, across thousands of image pixels within each quadrat. For each quadrat, we extracted all valid pixels from the orthomosaic (five bands: Blue, Green, Red, Red-edge, NIR). CV was calculated for each band across all valid pixels and then averaged across the five bands. Entropy was calculated for every pixel from its five-band probability vector and then averaged across pixels. All unique pixel pairs were used to form SAM angles, and then the mean angle is the quadrat-level SAM. These steps were also repeated for the VIS (RGB), RE-NIR (Red-edge + NIR), and all five-band combinations to mirror the hyperspectral windows.

2.4.2. Texture feature variables

We examined spatial variability within each 1 m × 1 m quadrat using second-order texture features derived from UAV imagery (Haralick et al., 1973). For every raster layer (five spectral bands), we generated a grey-level co-occurrence matrix (GLCM). Texture was quantified in a moving window of 3 × 3 pixels. Within each moving window, we generated four orientations (0°, 45°, 90°, 135°) with a one-pixel offset and averaged to produce a single, directionally invariant GLCM, as recommended by Haralick et al. (1973). From these averaged GLCMs, we calculated four texture feature variables, contrast, correlation, energy, and homogeneity, to characterize the fine-scale spatial patterns of vegetation and ground cover in four directions. These texture features were calculated for individual spectral bands, providing insights into the structural complexity and heterogeneity of the quadrats.

2.4.3. Structural diversity variables

To test the HVH, we calculated structural diversity metrics directly from the CHM rasters. Although our goal was to mirror the diversity variables used in the spectral analysis, the single-band nature of the CHM data limited our options. We therefore computed the CV to summarize the overall distribution of canopy heights and Shannon's Entropy to quantify the height distribution. Since only one band was available, we could not calculate SAM; instead, we introduced a structural richness metric, defined as the number of distinct, non-zero height values within each quadrat. This approach allowed us to evaluate structural diversity while acknowledging the constraints of the CHM data.

2.5. Data analysis and machine learning modelling

2.5.1. Continuum removal technique

To better understand the spectral characteristics of the ground cover types, we processed the collected pure spectral data. We refined the spectral data collected from various ground textures by first removing noisy wavelength ranges and then applying a continuum-removal technique to highlight key spectral features. After loading the raw reflectance measurements and omitting predefined noisy intervals, we transformed each spectrum using a Savitzky–Golay filter for smoothing, followed by a convex hull approach for continuum removal (Clark and Roush, 1984). This process normalized the spectra, allowing us to compare subtle differences in spectral signatures more effectively. We performed these steps for each ground cover type, calculated mean spectra, and visually compared both original and continuum-removed reflectance curves.

2.5.2. Statistical analysis

To evaluate the relationships between proximal, remotely sensed spectral, structural, and texture-based diversity and biodiversity variables, we employed Pearson's correlation analysis for the full dataset across years, months, and gardens. To account for differing phenological stages between 2021 and 2022, we then applied temporal analysis: (1) yearly correlations were computed separately for each year (Fig. S2); (2) monthly scatterplots of the top predictor-biodiversity pairs were produced to visualize intra-seasonal trends alongside overall annual regression lines (Fig. S3). The statistical significance of these relationships was assessed using p-values, with

standard thresholds applied to indicate varying levels of significance (* for $p < 0.05$, ** for $p < 0.01$, and *** for $p < 0.001$). This approach allowed us to determine both the strength and direction of the observed associations.

2.5.3. Remote and proximal sensing data integration and machine learning model development

We evaluated the predictive capabilities of various spectral, structural, and texture-based diversity variables to estimate biodiversity. As described in Section 2.4, we assembled multiple datasets incorporating different sets of predictors (e.g., hyperspectral, multispectral, structural, and texture features) and processed these datasets to ensure consistency and quality.

Our approach involved a systematic process of feature selection, model tuning, and validation to ensure robust and comparable results. After handling missing values and normalizing all numerical data using a Standard Scaler, we applied Recursive Feature Elimination with Cross-Validation (RFE) to identify the most performing feature for each biodiversity variable (Grabska et al., 2020; Zhang and Yang, 2020). RFE used a Random Forest Regressor (random_state = 42) as the estimator, with 5-fold cross-validation, where the dataset is divided into five equal parts. The model trains on four folds and validates on the fifth, repeating this process five times, so each fold serves as the validation set once. Mean squared error (MSE) was used as the scoring metric, iteratively removing one feature per step until the subset with the lowest mean squared error was identified. The final selected features for each biodiversity metric are listed in Tables S2 and S3.

For model development, we employed three regression approaches: Partial Least Squares Regression (PLSR), Multiple Linear Regression (MLR), and Random Forest Regression (RFR). For PLSR, the number of components was tuned via 5-fold cross-validation to minimize MSE, thereby optimizing model complexity and predictive accuracy. MLR was implemented with default parameters as a baseline, assuming linearity without explicitly validating assumptions such as homoscedasticity. RFR hyperparameters, including the number of trees, maximum depth, and minimum samples to split, were optimized using grid search with 5-fold cross-validation to effectively capture non-linear relationships in the data. Detailed parameter settings and performance metrics are provided in Table S1.

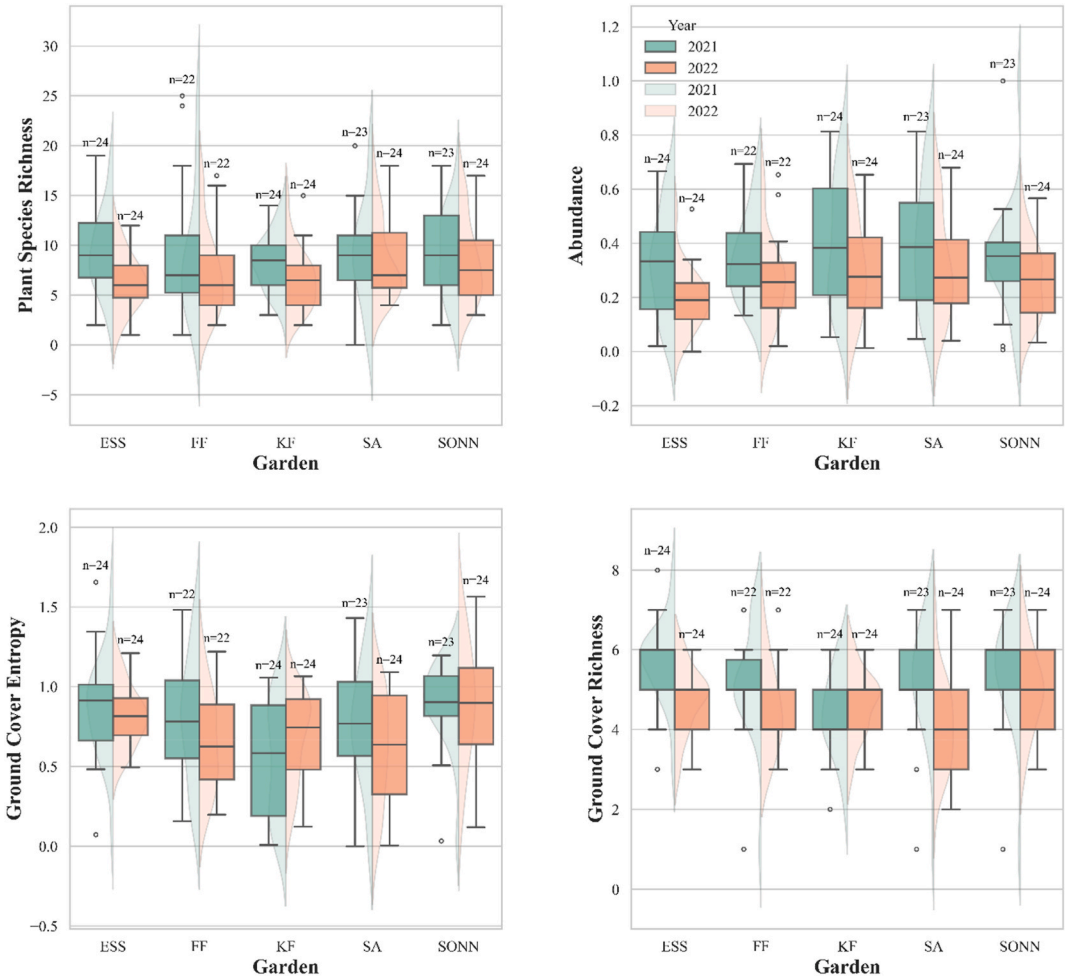

Fig. 4. Variation in plant species richness, abundance, ground cover entropy, and ground cover richness achieved from survey data across five urban community gardens, Essbare Stadt (ESS), Freihamer Freiluftgarten (FF), Karlsfeld (KF), StadtAcker (SA), and Sonnengarten Solln (SONN) in 2021 and 2022.

2.5.3.1. Data partitioning and resampling strategy. To evaluate model generalizability, we applied a repeated random hold-out protocol, randomly selecting 80 % of the dataset for training and reserving 20 % as an unseen test set across 20 independent iterations (random seeds 1 to 20). This repeated hold-out approach is essentially a form of Monte Carlo cross-validation (Picard and Cook, 1984), wherein the data are randomly partitioned into training (80 %) and testing (20 %) subsets without replacement in each iteration. Such repeated random subsampling is a simple and effective way to assess model performance, providing robust estimates by averaging results over multiple independent splits. Unlike a single train-test split or a traditional k-fold cross-validation (which uses fixed folds), this approach exposes the models to a variety of training-testing configurations, reducing the chance that results are dependent on any one particular partition of the data (Shan, 2022). The full data set comprises two years (2021 and 2022), five community gardens, and three sampling rounds per year (e.g., May, July, October in 2022). Repeating the split twenty times ensures that every garden × year × sampling-round combination appears several times in both training and test folds. This approach mitigates the risk of a single split scenario, such as focusing on a specific garden-year-month combination, achieving balanced representation without strict stratification.

Model performance was assessed using the coefficient of determination (R^2), root mean square error (RMSE), and normalized RMSE (NRMSE), calculated as RMSE divided by the range of observed values. For each predictor group (multispectral, hyperspectral, texture feature, and structural diversity variables, or their combination) and biodiversity variables combination, these statistical variables are calculated once per iteration on the independent 20 % test subset. The R^2 reported in Table 3 is the mean of the 20 single-fold R^2 values, not an R^2 recalculated on the pooled data. This practice follows the Monte-Carlo cross-validation, providing both a central estimate (mean) and an uncertainty interval (±SD) over independent resamples. However, the scatter points in Figs. 8–10 pool all 20 test predictions.

We first trained the models using individual predictor sets, including proximal hyperspectral, UAV-based multispectral, texture features, and structural diversity variables. Subsequently, we combined spectral diversity from multispectral imagery with texture features and structural diversity metrics to evaluate their combined contributions, focusing on horizontal variations (texture features) and vertical variations (structural diversity). Proximal hyperspectral variables were excluded to maintain consistency in data sources and emphasize remotely sensed variables. However, we also combined proximal hyperspectral data with multispectral imagery to explore the impact of higher spectral resolution (hyperspectral) and broader spatial coverage (multispectral) on biodiversity monitoring (see Fig. 3).

3. Results

3.1. Spatial and temporal variability of biodiversity variables

The analysis of biodiversity variables across five urban gardens (ESS, FF, KF, SA, and SONN) over two years (2021 and 2022) reveals notable trends in biodiversity variables (Fig. 4, Table 2). These differences were visually evident in comparisons of biodiversity variables (Fig. 4). Plant species richness and abundance varied between years, while the structural attributes of ground cover showed spatial variability among gardens. Such patterns highlight the interplay of temporal factors (e.g., seasonal management, weather conditions) and garden-specific management practices in shaping urban biodiversity. Notably, ground cover richness is the only variable changing by year and garden in our study. Additionally, Fig. 4 illustrates the range of each variable in different gardens and years in our dataset. For example, the KF showed the highest range of Abundances and Ground Cover Entropy in 2021; however, this did not remain consistent in the second year, suggesting that such variability was not inherent to the garden itself but rather changed during the second round of data collection. The changes observed across different years could be attributed to variations in garden management decisions made by the gardeners. These findings highlight the complexity of factors influencing urban garden biodiversity.

3.2. Ground cover composition and spectral characteristics

Ground cover composition exhibited marked heterogeneity, with herbaceous vegetation dominating (48.3 %), followed by bare soil (32.2 %) and grass (13.9 %). Minor yet ecologically relevant components included rock (5.3 %), leaf litter (4.2 %), woodchips (2.6 %), and wood (2.0 %), while the “others” and straw each contributed about 1.1 % (Fig. 5). The large error bars for some ground cover types, like herbs, reflect their natural variability across the randomly selected 1 × 1 quadrats, ranging from 0 % to 100 %, highlighting the heterogeneity of urban garden ecosystems rather than data inconsistencies. The considerable variability in herbaceous and bare

Table 2
Two-way ANOVA testing the effect of garden, year, and their interaction on ground survey-based biodiversity variables.

Variable	Garden	Year	Interaction (Garden & Year)
	P-value	P-value	P-value
Plant Species Richness	0.469	0.003 **	0.586
Abundance	0.064	0.000 ***	0.925
Ground Cover Entropy	0.000 ***	0.344	0.179
Ground Cover Richness	0.004 **	0.000 ***	0.037*

***, $p < 0.001$; **, $p < 0.01$; *, $p < 0.05$.

Table 3
Predictive performance of diversity-based predictor sets for each biodiversity variable. Predictor sets include hyperspectral, multispectral, texture features, structural metrics, and their integrated combinations. Performance statistics are reported as the coefficient of determination (R^2), root mean square error (RMSE), and normalized root mean square error (NRMSE), representing the best-performing models identified in Figs. 8–10. Values are the mean of the 20 fold-specific R^2 scores (not recomputed on the pooled points).

Biodiversity variables	Plant species richness			Abundance			Ground cover entropy			Ground cover richness		
	R^2	RMSE	NRMSE	R^2	RMSE	NRMSE	R^2	RMSE	NRMSE	R^2	RMSE	NRMSE
Hyperspectral	0.06	4.16	0.17	0.34	0.16	0.16	0.17	0.30	0.18	0.06	1.15	0.16
Multispectral	0.02	4.37	0.17	0.34	0.16	0.16	0.33	0.30	0.19	−0.01	1.30	0.22
Texture Features	0.03	4.92	0.20	0.20	0.15	0.16	0.14	0.34	0.23	−0.07	1.46	0.24
Structural	0.01	4.17	0.19	0.10	0.17	0.17	−0.03	0.36	0.23	−0.13	1.21	0.20
Multispectral + Texture	−0.01	4.43	0.18	**0.37**	**0.14**	**0.14**	0.20	0.32	0.21	0.04	1.24	0.21
Multispectral + Structural	0.07	4.13	0.17	**0.40**	**0.14**	**0.18**	**0.34**	**0.29**	**0.19**	0.03	1.20	0.2
Hyperspectral + Multispectral	0.10	4.42	0.18	**0.42**	**0.14**	**0.14**	**0.39**	**0.29**	**0.18**	0.06	1.18	0.20

soil coverage suggests microhabitat differences potentially influencing nutrient cycling, soil stability, and resource availability for pollinators and other fauna.

Spectral measurements (350–2350 nm) revealed distinct reflectance patterns between vegetative (herb, grass) and non-vegetative (bare soil, stone, wood, litter, straw, woodchip) materials (Fig. 6). Vegetation showed strong chlorophyll absorption in the visible range (400–700 nm) and high NIR reflectance (750–1350 nm), indicative of healthy foliar structures. SWIR absorptions related to water content and biochemical constituents (lignin, cellulose) were prominent in herbaceous materials. Non-vegetative covers exhibited lower NIR reflectance and characteristic SWIR features tied to mineralogical or lignocellulosic compositions. Bare soil and stone showed gradual reflectance increases in the visible to NIR range, reflecting mineralogical properties, while wood and woodchip demonstrated distinct SWIR absorptions due to cellulose and lignin. Litter and straw exhibited intermediate spectral patterns, combining traits of both vegetative and non-vegetative components.

3.3. Spectral diversity and biodiversity relationships

The three spectral diversity metrics (CV, SAM, and Entropy) produced varying outcomes depending on the selected diversity variables, spectral regions, and sensor types (Fig. 7a and b). Their relationships with biodiversity variables, including Plant Species Richness, Abundances, Ground Cover Entropy, and Ground Cover Richness, differed accordingly. Consequently, the performance of

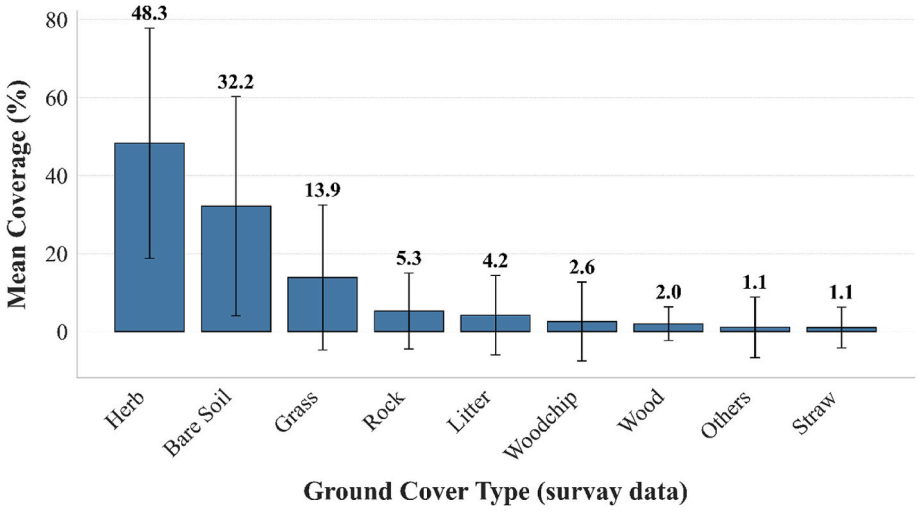

Fig. 5. Mean percentage cover (± standard error) of ground cover types (herb, grass, bare soil, rock, litter, woodchip, wood, others, straw) across the urban gardens in 2021 and 2022.

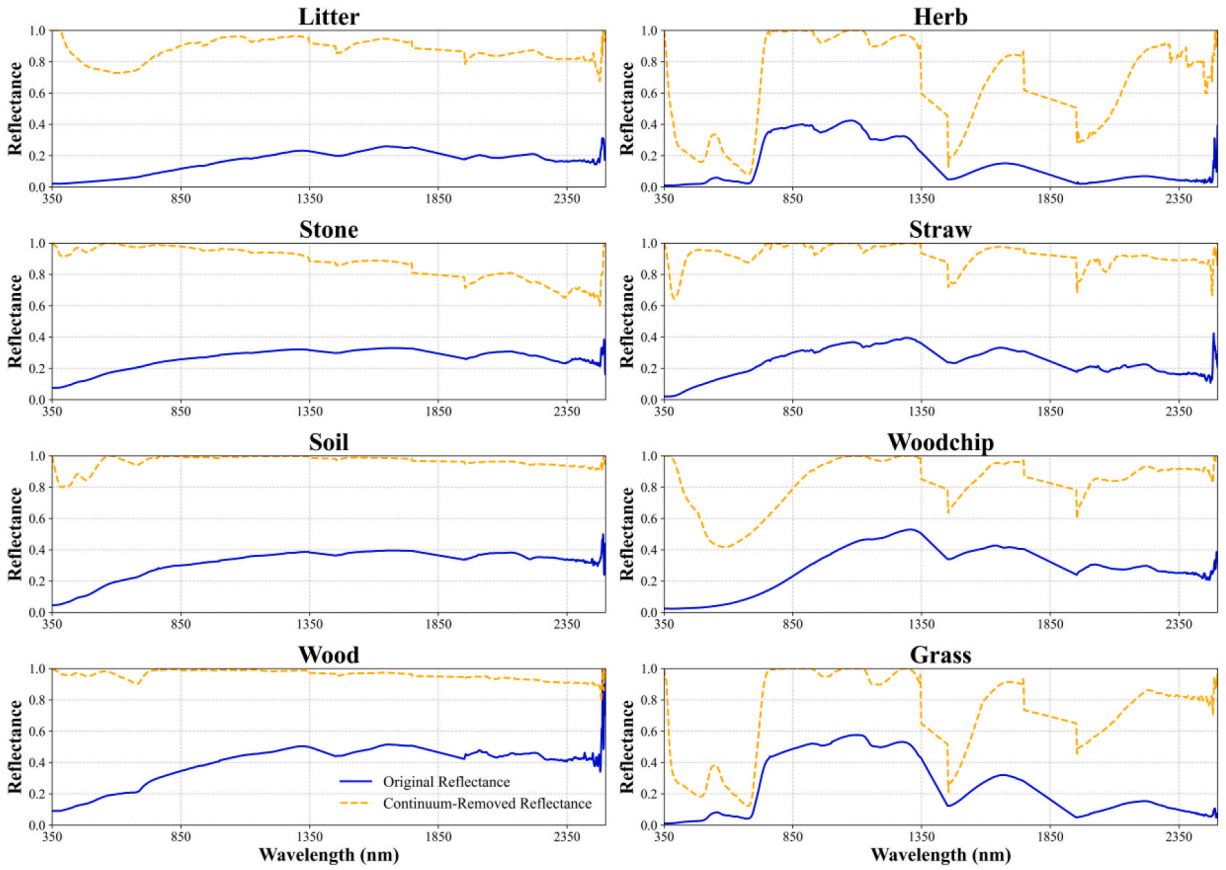

Fig. 6. Continuum-removed reflectance spectra for various ground cover types using the Convex Hull method. Original reflectance (Blue solid line) and continuum-removed (yellow dash line) spectra emphasize unique reflectance and absorption regions.

spectral diversity metrics can be categorized into two distinct groups; 1) across all spectral regions, 2) across different spectral regions. In this section, we highlight the most important artefacts.

Firstly, across all spectral regions, the spectral diversity variables SAM and Entropy, calculated from both hyperspectral and multispectral data, demonstrated the most significant negative correlations with plant diversity variables, with the absolute highest correlation coefficients of $r = -0.36$ and $r = -0.61$, respectively ($p < 0.01$). This finding aligns with previous research (Gholizadeh et al., 2018), which suggests that the exposure of non-vegetative components (specifically soil) whose spectral reflectance markedly differs from those of vegetative parts, can lead to significant negative correlations with plant species richness. Moreover, Spectral Entropy decreases with more plant diversity (Plant Species Richness, and Abundances) by capturing spectral complexity from non-vegetative parts. In general, the relationships between hyperspectral data and plant diversity variables (Plant Species Richness and Abundances) were weaker compared to multispectral data. We speculate that the weaker correlation arises from the fact that hyperspectral diversity variables were calculated using the entire spectrum, many of which might not strongly correlate with plant diversity (Gholizadeh et al., 2018). This broad inclusion likely dilutes the relationship, leading to a reduced correlation. Notably, all spectral diversity variables derived from hyperspectral data and multispectral imagery exhibited a positive linear relationship with Ground Cover Entropy. When considering all the bands, Ground Cover Richness showed the best relationship with SAM in the multispectral data analysis and CV in the hyperspectral.

Secondly, we evaluated the contribution of single bands and the combination of bands in separated spectral regions (VIS, Red-edge-NIR, and SWIR bands). Among the single bands, CV in the blue wavelength exhibited a significant positive correlation with Abundances ($r = 0.21$ and $r = 0.28$ for hyperspectral and multispectral, respectively) (Fig. 7a and b). In contrast, CV in the Red-edge and NIR bands showed negative correlations with both plant diversity variables in multispectral data, but were positively correlated with Ground Cover Entropy, in both multi- and hyperspectral data analysis ($p < 0.01$). Moreover, they showed a significant relationship with Ground Cover Richness only in hyperspectral. Additionally, our analysis demonstrated that different spectral regions contributed uniquely to biodiversity variation. The VIS bands generally showed modest positive relationships with biodiversity variables for CV and SAM. However, the observed drop in correlation (r) for both multi- and hyperspectral CV against Abundances suggests that including the green and red portions of the spectrum might have adversely affected the relationship compared to using only the blue bands. Conversely, the Red-edge-NIR region consistently produced non-significant correlations for both CV and SAM vs. plant diversity variables, but in contrast, they were successful in capturing Ground Cover Entropy (multi- and hyperspectral) and Richness (only

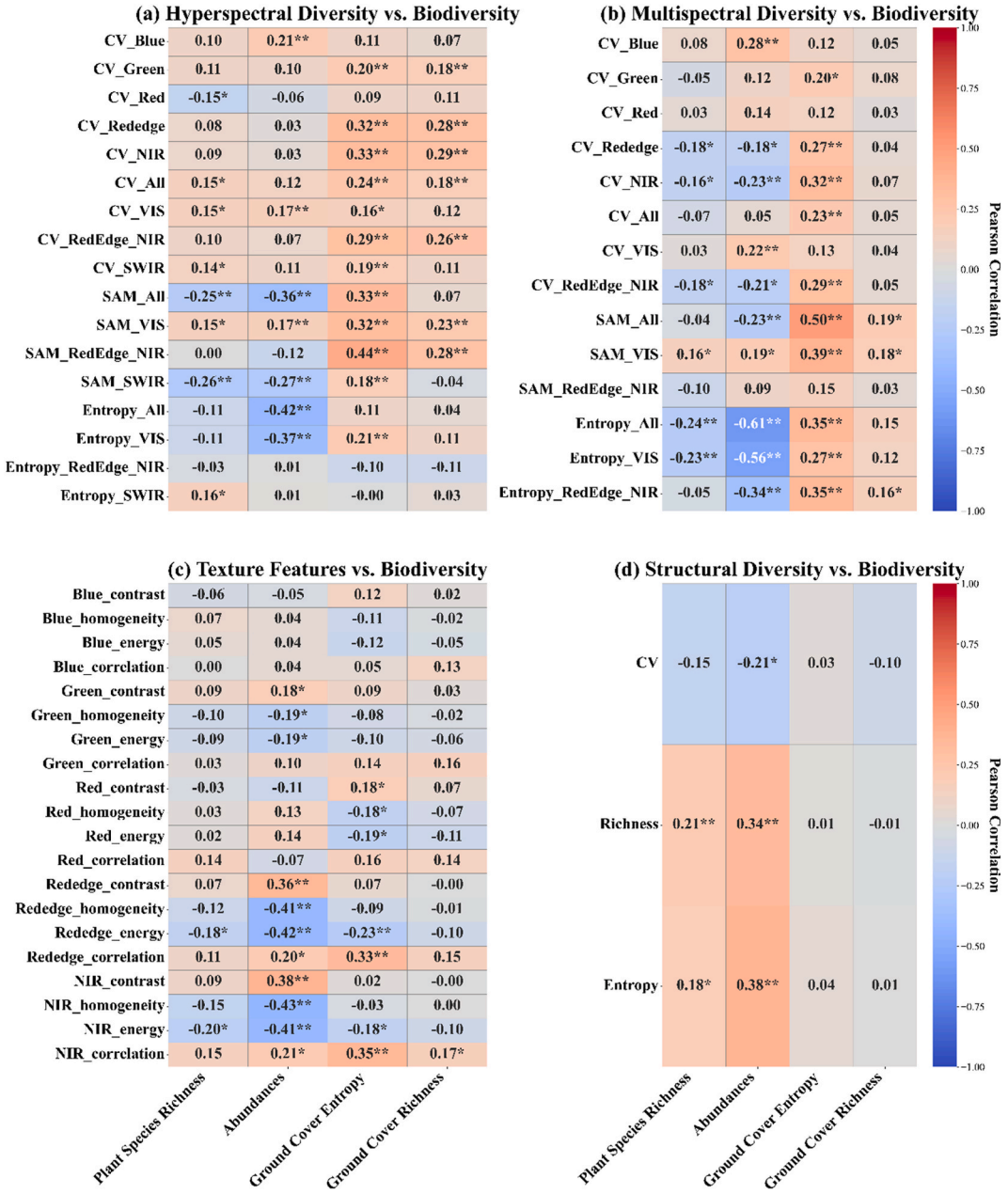

Fig. 7. Pearson correlation coefficients between biodiversity metrics (plant species richness, abundances, ground cover entropy, and richness) and spectral, texture, and structural diversity metrics. Colour gradients indicate the strength and direction of correlations. ***, $p < 0.001$; **, $p < 0.01$; *, $p < 0.05$.

hyperspectral). In addition, entropy calculated from VIS bands was negatively associated with plant diversity while positively correlating with Ground Cover Entropy, indicating its sensitivity to the presence of non-vegetative elements that influence spectral complexity. The SWIR bands yielded mixed results; they occasionally enhanced the discrimination of plant diversity but did not consistently produce statistically robust correlations. This inconsistency is likely attributable to the SWIR bands' heightened sensitivity to water content, which may introduce variability not directly related to biodiversity.

3.4. Contribution of texture feature and structural diversity to biodiversity variables

Texture features revealed significant associations with biodiversity indicators (Fig. 7c), specifically in the red edge and NIR portions of the spectrum. NIR_correlation positively correlated with Ground Cover Entropy ($r = 0.35$, $p < 0.01$), Abundances ($r = 0.21$, p

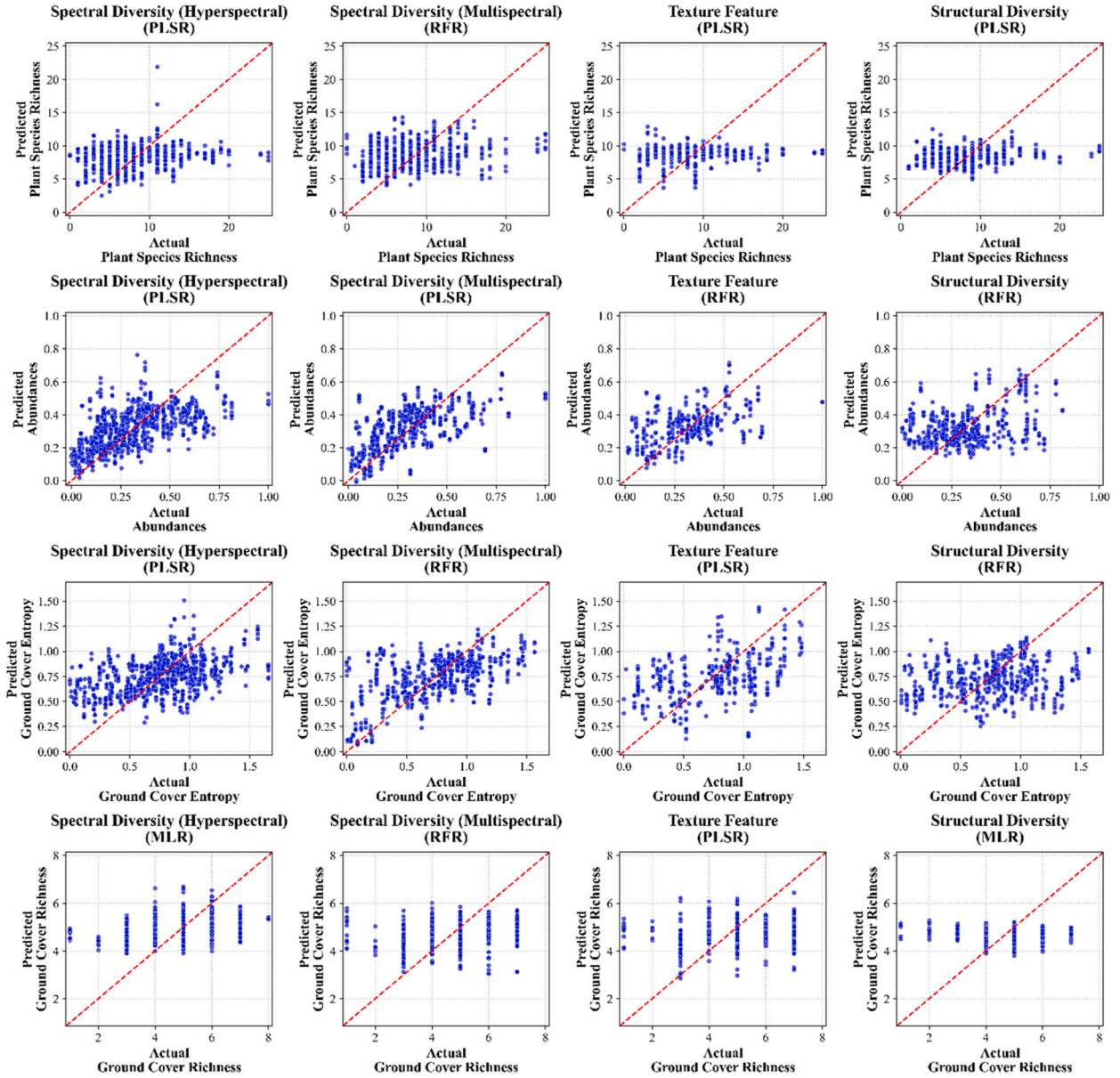

Fig. 8. Predictive performance of diversity variables (hyperspectral, multispectral, texture feature, and structural) and biodiversity variables, including plant species richness, abundance, ground cover entropy, and ground cover richness. Scatter plots compare remotely sensed predictions to actual values using regression models: Partial Least Squares Regression (PLSR), Random Forest Regression (RFR), and Multiple Linear Regression (MLR). Each scatter plot shows a scatter of all test-set predictions from 20 iteration Monte-Carlo (80/20) splits for a specific remote sensing diversity, biodiversity variables combination. The red dashed line represents the 1:1 relationship, illustrating the alignment between predicted and observed values.

< 0.05), and the highest absolute correlation ($r = 0.17$, $p < 0.05$) with Ground Cover Richness, implying that regions with higher structural variability in ground cover have more variable textures in this spectral band. Red-edge correlation showed strong links to Ground Cover Entropy ($r = 0.32$, $p < 0.01$) and abundances ($r = 0.20$, $p < 0.05$), which suggests that red edge is less susceptible to the richness of the ground cover. Conversely, homogeneity metrics in the green and NIR bands negatively correlated with abundance (e.g., NIR_homogeneity: $r = -0.43$, $p < 0.001$), indicating less diversity in spectrally uniform areas. This suggests that areas with more homogenous textures in these bands are associated with lower Abundances, potentially reflecting more uniform, less densely vegetated areas. Among the visible-band texture features, only the green band showed a significant relationship with Abundances, which was due to its sensitivity to the variability of green vegetation cover. These results underscore the ability of texture features, particularly from NIR and red-edge bands, to capture structural and compositional variability in urban biodiversity.

Structural Richness is positively correlated with both Plant Species Richness ($r = 0.21$, $p < 0.01$) and Abundances ($r = 0.34$, $p <$

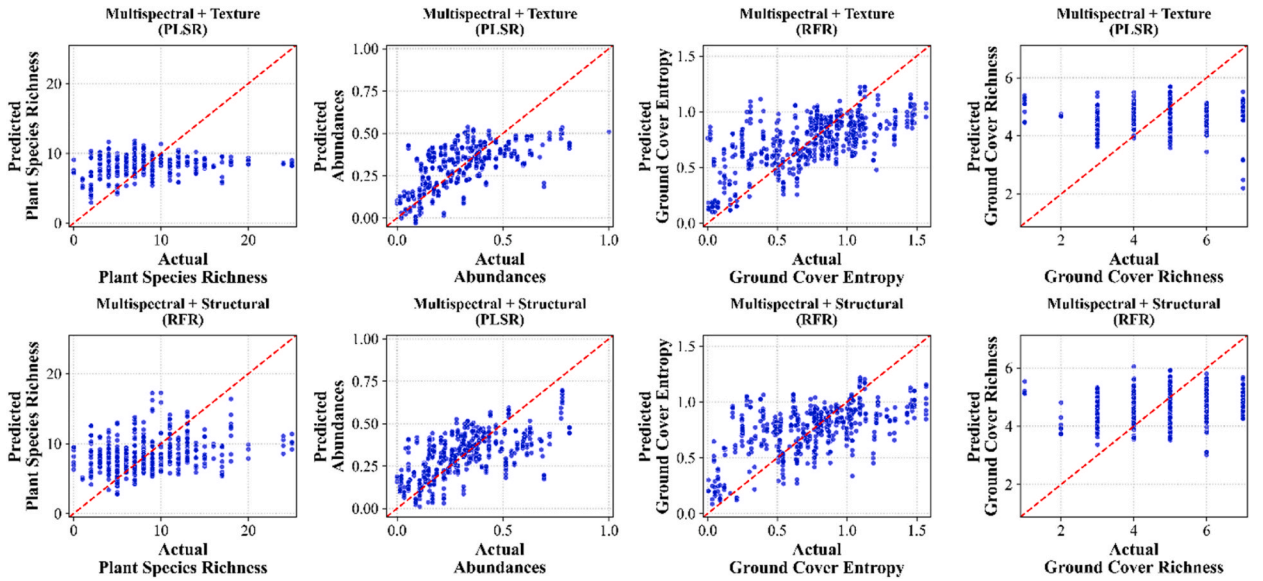

Fig. 9. Predictive performance of integrated remotely sensed diversity variables (multispectral, texture, and structural) for biodiversity assessment using Partial Least Squares Regression (PLSR) and Random Forest Regression (RFR). Each scatter plot shows a scatter of all test-set predictions from 20 iteration Monte-Carlo (80/20) splits for a specific remote sensing diversity, biodiversity variables combination. The red dashed line represents the 1:1 relationship between predicted and actual values.

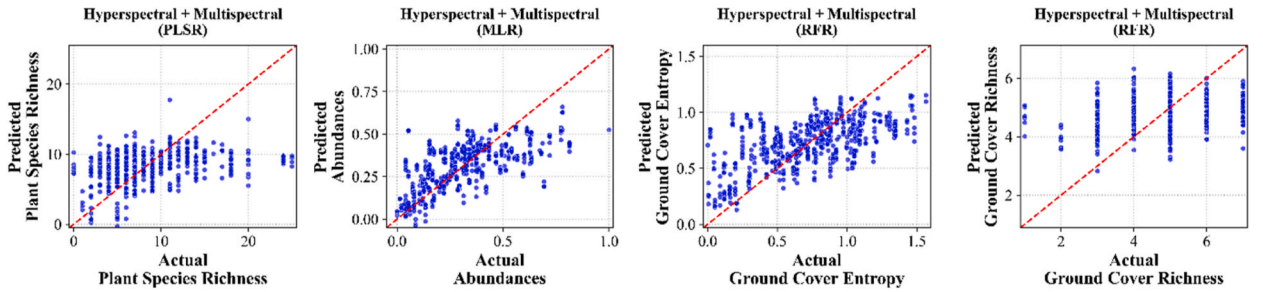

Fig. 10. Predictive performance of combined proximal hyperspectral and remotely sensed multispectral diversity variables for biodiversity using regression models: Partial Least Squares Regression (PLSR), Random Forest Regression (RFR), and Multiple Linear Regression (MLR). Each scatter plot shows a scatter of all test-set predictions from 20 iteration Monte-Carlo (80/20) splits for a specific remote sensing diversity, biodiversity variables combination. The red dashed line represents the 1:1 relationship, illustrating the alignment between predicted and observed values.

0.01), suggesting that areas with greater structural diversity support more diverse and abundant plant communities. Similarly, structural Entropy exhibited positive correlations with Plant Species Richness ($r = 0.18$, $p < 0.05$) and Abundances ($r = 0.38$, $p < 0.01$), further indicating that structurally complex areas tend to harbour higher biodiversity. This aligns with ecological theories that structurally heterogeneous plant populations provide more resources and habitats, thus supporting the diversity of creatures (Farwell et al., 2021). In contrast, structural CV showed negligible correlations with Plant Species Richness ($r = -0.15$, $p > 0.05$) in this analysis, while it had a negative significant correlation ($r = -0.21$, $p < 0.05$) with Aboundances. The structural diversity metrics did not show any significant correlations against ground cover diversity variables. This was logical, because the structural metrics are calculated based on object height, and most of the ground covers have zero or close to zero height compared to plants.

3.5. Machine learning-based biodiversity assessment using spectral and structural diversity variables

3.5.1. Biodiversity estimation using individual spectral, structural, and texture feature variables

The predictive capabilities of spectral and structural diversity for biodiversity variables were evaluated using multiple regression approaches, and the best model for each plant and ground diversity metric is illustrated (Fig. 8, Tables S1 and 2, Fig. S4).

Hyperspectral diversity metrics provided the highest predictive accuracy, yet relatively weak, for Plant Species Richness ($R^2 = 0.09$; RMSE = 3.92; NRMSE = 0.16) when modeled using PLSR, capturing subtle spectral variations associated with species composition compared to the other diversity metrics. Multispectral ($R^2 = 0.02$; RMSE = 4.37; NRMSE = 0.17) and texture features ($R^2 = 0.03$; RMSE = 5.06; NRMSE = 0.2) exhibited weaker correlations, while structural diversity metrics were minimally predictive (R^2

= 0.01; RMSE = 4.17; NRMSE = 0.19). The reason for this lies in the fact that different plant species in an urban community garden have only minor effects on reflectance and exhibit limited structural differences.

Hyperspectral and multispectral diversity variables demonstrated the strongest predictive performance for abundance ($R^2 = 0.34$; RMSE = 0.16; NRMSE = 0.16), particularly when modeled using PLSR. Texture features ($R^2 = 0.20$; RMSE = 0.15; NRMSE = 0.16) also provided robust predictions, capturing both spectral and spatial variability in vegetation structure. In contrast, structural diversity metrics showed weaker predictive power ($R^2 = 0.10$; RMSE = 0.17; 0.17), indicating reduced sensitivity to abundance variations.

Ground Cover Entropy predictions were also best explained by multispectral diversity ($R^2 = 0.33$; RMSE = 0.3; NRMSE = 0.19), followed by hyperspectral diversity ($R^2 = 0.17$; RMSE = 0.30; NRMSE = 0.18). Texture feature variables provided comparatively moderate predictive capacity ($R^2 = 0.14$; RMSE = 0.34; NRMSE = 0.23). Structural diversity metrics displayed weak predictive power ($R^2 = -0.03$; RMSE = 0.36).

Ground Cover Richness showed limited predictive performance across the diversity variable groups. Hyperspectral diversity ($R^2 = 0.06$; RMSE = 1.15; NRMSE = 0.16) exhibited the highest predictive capacity among the tested groups, although still weak.

3.5.2. Integrated diversity variables for biodiversity assessment

Combining multispectral diversity with texture features moderately improved the predictive performance for abundances ($R^2 = 0.37$; RMSE = 0.14; NRMSE = 0.14). However, this combination did not significantly enhance predictions for ground cover entropy ($R^2 = 0.20$; RMSE = 0.32; NRMSE = 0.21) and, similar to the previous step (Fig. 8), exhibited limited predictive capacity for plant species richness and ground cover richness (Fig. 9, Tables S1 and 3, Fig. S5).

The integration of multispectral and structural metrics resulted in the highest predictive performance for Abundances ($R^2 = 0.40$; RMSE = 0.14; NRMSE = 0.18), modeled with PLSR. This combination leveraged both broad spectral sensitivity and structural diversity, effectively capturing patterns in vegetation distribution and Abundances. Ground cover entropy predictions showed a modest improvement when multispectral and structural diversity metrics were combined ($R^2 = 0.34$; RMSE = 0.29; NRMSE = 0.19). However, the integration of these variables demonstrated limited success in predicting plant species richness and ground cover richness. The findings indicate that variations in plant species and ground cover types impact spectral and structural variables, depending on whether the background is vegetative or non-vegetative.

Across all biodiversity variables, combining proximal hyperspectral and remotely sensed multispectral diversity variables outperformed single-dataset models, particularly for predicting abundances ($R^2 = 0.42$; RMSE = 0.15; NRMSE = 0.15) and ground cover entropy ($R^2 = 0.39$; RMSE = 0.29; NRMSE = 0.18) (Fig. 10, Tables S1 and 3, Fig. S5).

4. Discussion

4.1. Spectral diversity–biodiversity relationship depends on spectral regions

Our findings confirm that spectral diversity variables, including CV, SAM, and Entropy, can provide valuable insights into biodiversity patterns. When applied to both proximal hyperspectral and drone-based multispectral imagery, these spectral diversity variables showed significant but often moderate positive correlations with ground cover diversity (particularly ground cover entropy), offering partial support for SVH (Hauser et al., 2021; Palmer et al., 2002). However, these relationships indicate that other factors, such as non-vegetative elements (soil, wood, woodchip, etc.), microclimate variations, or management practices, likely contribute to ground cover diversity in urban community gardens.

The positive relationship between spectral diversity and plant diversity was not always consistent. This relationship can be different in highly heterogeneous urban environments, such as community gardens, due to the complex interplay of vegetative and non-vegetative components. More vegetation leads to a more homogeneous reflectance, rich in chlorophyll and similar structural features, thus reducing spectral variability (Asner and Martin, 2008).

Our result underscores the importance of targeted spectral regions for ecological and remote sensing applications, emphasizing that specific wavelengths might effectively capture spectral diversity variation related to different characteristics and traits. A key outcome of our study is the identification of specific spectral regions that are more effective at capturing biodiversity-related variation. Our results demonstrate that focusing on non-visible spectral bands, particularly in the Red-edge (approximately 690–760 nm) and Near-Infrared (NIR; approximately 760–1300 nm) domains, enhances the detection of structural and compositional heterogeneity in ground cover. This spectral range could partly be covered in the UAV multispectral bands. These regions are sensitive to leaf biochemical and canopy structural traits (e.g., chlorophyll content, leaf area index) and moisture content, resulting in stronger contrast between vegetative and non-vegetative substrates (Danner et al., 2017; Luis Hernández-Stefanoni et al., 2012). Notably, Red-edge and NIR bands consistently outperformed visible bands (e.g., red, green, blue) in capturing ground cover diversity, underscoring their potential for improving ecological characterization in heterogeneous urban garden environments. It is crucial to acknowledge that the ground cover diversity variables used in this study were derived from a mixture of different ground cover types. Therefore, these findings may not apply to every combination of ground-cover types. Considerable spectral dissimilarities between vegetation (herb and grass) and soil are evident in several studies (Hauser et al., 2021; Wang et al., 2018).

Looking at plant diversity variables, we observed contrasting patterns. In scenarios where non-vegetative parts are also exposed, spectral diversity variables that rely on visible-range wavelengths (~400–700 nm) showed stronger associations with plant species richness and abundance than those relying on Red-edge and NIR domains (Gholizadeh et al., 2018). This pattern can be attributed to the influence of leaf pigments and chlorophyll absorption features, which are more pronounced in the visible range and directly affect reflectance variability among vegetated surfaces (Knipling, 1970; Rouse et al., 1974; Zeng et al., 2020). This trend works well for

CV_VIS and SAM_VIS. However, spectral entropy (e.g., Entropy_VIS, Entropy_All) demonstrated a contrasting trend. Spectral entropy focuses on the relative distribution of reflectance values across wavelengths but does not account for how far apart those values are. This distinction becomes particularly relevant in vegetation-dominated areas, where the reflectance values across wavelengths tend to converge due to shared features like chlorophyll absorption and similar canopy structures (Rocchini et al., 2017). Even though reflectance values might still vary across wavelengths, the dominance of vegetation features skews the distribution, leading to lower spectral entropy. These results suggest that while spectral entropy can offer unique insights into vegetation patterns, it may be less effective in capturing the diversity of vegetation in areas with high vegetative dominance.

4.2. The role of texture features and structural diversity in explaining biodiversity

Drone multispectral texture features were explored due to their sensitivity to similarity or dissimilarity between adjacent pixels and spatial heterogeneity (Haralick et al., 1973). In general, texture features were more correlated to Abundances, likely due to their capacity to capture vegetation configuration in three dimensions, while it is moderately correlated with compositional heterogeneity (Farwell et al., 2021; O'Brien et al., 1995). The informative regions of the spectrum for estimating biodiversity through texture features varied significantly. Texture features derived from Red-edge and NIR bands showed the highest correlation, likely due to the greater sensitivity of these bands to the vertical variability of vegetation structure compared to VIS bands (Farwell et al., 2021). Moreover, the enhanced differences in spectral reflectance from vegetative parts and the suppression of reflectance from non-vegetative parts in these bands may improve the discrimination of different ground covers while minimizing bias introduced by aerosols (Erlandsson et al., 2023; Hofmann et al., 2017; Madonsela et al., 2017).

The statistically significant but weak positive relationship between structural richness and entropy with plant diversity variables partially supports the HVH (Torresani et al., 2020). Specifically, plant abundances exhibited a stronger correlation with structural diversity than plant species richness, suggesting that total abundances contain more vegetation structural information (O'Brien et al., 1995). Conversely, the structural CV, which emphasizes the relative height variation, decreased as abundances increased, indicating greater height uniformity. Additionally, we did not observe a significant association between structural diversity and ground cover diversity (GCE and GCR) as anticipated. This lack of association likely stems from the limitations of the canopy height model used as the base map for calculating structural diversity, which is less effective in capturing variations in predominantly flat ground cover types.

4.3. Improved assessment of biodiversity by combining spectral and structural diversity variables

The predictions for Plant Species Richness and Ground Cover Richness showed consistently weak performance across all ML models. This may be attributed to the distinct characteristics of urban community gardens, which are dominated by herbs, bare soil, and grass, as expected in horticultural systems focused on plant production. Unlike densely vegetated ecosystems such as forests or grasslands, urban community gardens have lower plant density and significant non-vegetative ground cover types, such as bare soil, woodchips, and mulch. These non-vegetative elements highly affect spectral diversity by capturing variability in surface roughness, moisture levels, and reflectance properties, which can overshadow the vegetation signal. This variability makes biodiversity richness metrics particularly challenging to predict in such heterogeneous environments.

In contrast to biodiversity richness-based (plant species richness and ground cover richness) prediction, ML models showed comparatively stronger prediction ability using spectral diversity for abundances (proximal hyperspectral and remote multispectral) and ground cover entropy (remotely multispectral diversity variables). The link between proximal hyperspectral diversity and ground cover entropy was weaker, likely because the 'point' spectral data collection did not fully cover the entire 1×1 quadrat, making it difficult to capture detailed spatial patterns. However, our results demonstrated that integrating hyperspectral and multispectral data enhances predictive accuracy, specifically for predicting abundances and ground cover entropy. This improvement is driven by the detailed spectral resolution of hyperspectral data and the spatial variability captured effectively by multispectral imagery.

When used individually, structural diversity variables derived from the canopy height models demonstrated limited predictive capacity for Abundances and Ground Cover Entropy. This underperformance may stem from two factors: (1) the reliance on fewer structural features compared to texture features and (2) the singular focus on height-based metrics, which do not fully capture the variability in vegetation structure. Texture features, derived from spectral data, outperformed structural diversity when used individually due to their ability to quantify the horizontal spatial heterogeneity (Zhu et al., 2024b).

Integrating spectral and structural features improved the prediction of abundances and ground cover entropy by leveraging complementary information. Interestingly, while texture feature variables, derived from spectral data, outperformed structural diversity when used individually in ML models, the combination of structural and spectral diversity proved more effective. Structural diversity, which captures vertical three-dimensional variations, complements spectral diversity by providing an additional perspective on ecosystem complexity. This synergistic integration provided a more holistic representation of ecosystem heterogeneity, enhancing predictive accuracy.

These findings highlight the potential of combining complementary diversity variables by providing a broader and more balanced representation of ecosystem complexity for biodiversity assessment. In urban community gardens, where heterogeneity and exposure of non-vegetative elements present unique challenges, leveraging both spectral and structural data offers a promising path forward. Overall, the stronger relationship between abundance and remote sensing diversity variables suggests that these metrics capture vegetation quantity and structural complexity more effectively than species richness, which remains difficult to measure reliably in heterogeneous urban gardens with remote sensing approaches. Future research should explore whether this integrative approach can

similarly enhance biodiversity predictions in other ecosystems, such as forests, grasslands, or agricultural landscapes.

4.4. Further work

This study utilized high spatial resolution multispectral images and point-based hyperspectral data to explore spectral diversity in complex urban community gardens. While these data provided valuable insights, it is important to acknowledge several limitations that may affect the generalizability and comprehensiveness of our findings.

First, the study was conducted in five urban community gardens in southern Bavaria, which might limit the applicability of the results to other urban environments with different vegetation types, management practices, and ground cover compositions. Urban garden biodiversity is influenced by local management practices and socio-cultural context, which differ across regions (M.H. Egerer et al., 2017; Lin and Philpott, 2015). Therefore, the unique ecological characteristics of Bavarian community gardens may not fully represent other urban gardens and ecosystems. Future research should explore similar approaches in diverse urban settings to test the proposed methods across various ecological and socio-cultural urban environments.

Second, although we considered four biodiversity variables, plant species richness, total plant abundances, ground cover entropy, and ground cover richness, other aspects of biodiversity, such as functional diversity and phylogenetic diversity, were not assessed. These dimensions are critical for understanding ecosystem functioning and resilience, as they capture the variety of ecological roles and evolutionary relationships among species (Flynn et al., 2011). The effectiveness of our remote sensing approach for capturing these additional biodiversity facets remains unknown, and future studies can incorporate these metrics to provide a more comprehensive assessment of urban garden ecosystems.

Third, concerning data resolution, the high-spatial resolution multispectral images (8–13 mm/px) and high-spectral resolution of point-based hyperspectral data (350–2500 nm) used in this study have been proven to be suitable for detecting broad patterns of spectral diversity. However, the low spectral resolution of multispectral imagery and the constrained spatial coverage of point-based hyperspectral measurements may not fully capture the fine-scale heterogeneity in small patches or subtle variations within plant canopies from the nadir view. An integrated LiDAR and hyperspectral imaging system might enable mapping such within-canopy heterogeneity (Zhu et al., 2024), although such a technique was not available in this study. Nonetheless, multi-model sensing data interpretation may have been constrained by non-explicitly georeferenced ground survey data (Getzin et al., 2012).

Additionally, temporal variability in management practices and seasonal changes likely introduced variability in ground cover and species compositions, which may have influenced our results. Urban gardens are dynamic systems shaped by human interventions, and our study captured only snapshots across two years (2021 and 2022). Our month-by-month analysis showed that biodiversity-spectral relationships occurred not only during peak vegetation growth (July to August) but also in early-season measurements (May) (Fig. S3), which could support pollinator-related monitoring; future work could include precipitation data to account for interannual variations. Longitudinal studies incorporating multi-temporal remote sensing data could better account for these dynamics and provide insights into the temporal stability of biodiversity patterns (Vihervaara et al., 2017). Such approaches would help assess the effects of seasonal changes and management decisions on biodiversity metrics.

Despite these limitations, the variations in spectral diversity variables still provide valuable insights into how urban gardens function on a larger scale (Wang and Loreau, 2016). For example, an area with rocks, soil, leaves, straw, and woodchips would have various ground covers. Although such diversity may support invertebrate richness, it may not favour pollination activities as a simple plot with only herbs and grasses. How each ground cover type contributes individually and synergistically to the functioning of gardens and their biodiversity is beyond the scope of the present study. However, our findings are valuable to remotely identifying animal habitat and nesting resources, such as ground-nesting bees, whose abundance and diversity may correlate with such field measurements (Cohen et al., 2020). Future research could build upon these findings by integrating additional biodiversity variables, employing higher resolution data, and accounting for temporal dynamics to further advance our understanding of urban garden ecosystems.

5. Conclusions

This study highlights the potential of integrating spectral and structural diversity variables for enhancing biodiversity assessments in highly heterogeneous urban community gardens. Our findings demonstrate that while red-edge and NIR ranges are more effective for capturing structural and compositional variability of ground cover, visible bands better reflect subtle differences in vegetation communities. Furthermore, texture features derived from multispectral imagery and structural diversity variables based on canopy height models provided valuable insights into canopy structural heterogeneity.

By combining the detailed spectral signals captured by point-based hyperspectral measurements with the drone multispectral imaged structural diversity metrics, we achieved stronger predictions for key indicators such as plant abundance and ground cover variety. This approach performs better than relying on a single data source, highlighting the importance of using complementary remote sensing data together to address the natural complexity found in urban green spaces.

CRediT authorship contribution statement

Yasamin Afrasiabian: Writing – review & editing, Writing – original draft, Visualization, Validation, Software, Methodology, Formal analysis, Data curation, Conceptualization. **Felix Contiz:** Writing – review & editing, Methodology, Data curation. **Elisa Van Cleemput:** Writing – review & editing, Supervision. **Monika Egerer:** Writing – review & editing, Supervision, Methodology, Funding acquisition, Data curation. **Kang Yu:** Writing – review & editing, Validation, Supervision, Software, Methodology, Funding

acquisition, Conceptualization.

Ethics in publishing statement

This research presents an accurate account of the work performed, all data presented are accurate and methodologies detailed enough to permit others to replicate the work.

This manuscript represents entirely original works and or if work and/or words of others have been used, that this has been appropriately cited or quoted and permission has been obtained where necessary.

This material has not been published in whole or in part elsewhere.

The manuscript is not currently being considered for publication in another journal.

That generative AI and AI-assisted technologies have not been utilized in the writing process or if used, disclosed in the manuscript the use of AI and AI-assisted technologies and a statement will appear in the published work.

That generative AI and AI-assisted technologies have not been used to create or alter images unless specifically used as part of the research design where such use must be described in a reproducible manner in the methods section.

All authors have been personally and actively involved in substantive work leading to the manuscript and will hold themselves jointly and individually responsible for its content.

Declaration of generative AI and AI-assisted technologies in the writing process

During the preparation of this work, the authors used ChatGPT to improve the language. After using this tool, the authors reviewed and edited the content as needed and take full responsibility for the content of the publication.

Declaration of competing interest

The authors declare that they have no known competing financial interests or personal relationships that could have appeared to influence the work reported in this paper.

Acknowledgements

This work was supported by the Hans Eisenmann-Forum für Agrarwissenschaften (HEF) Seed Fund 2021. The authors sincerely and wholeheartedly were thankful to help of Ali Mokhtari, Jürgen Pluss, Jie wang, Haibo Yang, Weilong Qin, Nina Schäle, Michael Miesl, Julia Schmack, Yannick Hecher, Veronica Sebald, Astrid Neumann, Hien Nguyen. We also thank the editor and the anonymous reviewer for their constructive and insightful comments.

Appendix A. Supplementary data

Supplementary data to this article can be found online at https://doi.org/10.1016/j.rsase.2025.101685.

Data availability

The authors do not have permission to share data.

References

Anderson, E.C., Avolio, M.L., Sonti, N.F., LaDeau, S.L., 2021. More than green: tree structure and biodiversity patterns differ across canopy change regimes in Baltimore's urban forest. Urban For. Urban Green. 65, 127365. https://doi.org/10.1016/J.UFUG.2021.127365.

Asner, G.P., Martin, R.E., 2008. Spectral and chemical analysis of tropical forests: scaling from leaf to canopy levels. Remote Sens. Environ. 112, 3958–3970. https://doi.org/10.1016/J.RSE.2008.07.003.

Asner, G.P., Martin, R.E., Anderson, C.B., Knapp, D.E., 2015. Quantifying forest canopy traits: imaging spectroscopy versus field survey. Elsevier. In: Asner, G.P., Martin, R.E., Anderson, C.B. (Eds.), KnappRemote Sens. Environ. 2015•Elsevier, pp. 15–27. https://doi.org/10.1016/j.rse.2014.11.011, 158.

Bellis, L.M., Pidgeon, A.M., Radeloff, V.C., St-Louis, V., Navarro, J.L., Martella, M.B., 2008. Modeling habitat suitability for greater rheas based on satellite image texture. Ecol. Appl. 18, 1956–1966. https://doi.org/10.1890/07-0243.1.

Clark, R.N., Roush, T.L., 1984. Reflectance spectroscopy: quantitative analysis techniques for remote sensing applications. J. Geophys. Res. 89, 6329–6340. https://doi.org/10.1029/JB089IB07P06329.

Cohen, H., McFrederick, Q.S., Philpott, S.M., 2020. Environment shapes the microbiome of the blue orchard bee, Osmia lignaria : RRH: environmental drivers of bee microbiome. Microb. Ecol. 80, 897–907. https://doi.org/10.1007/S00248-020-01549-Y.

Danner, M., Berger, K., Wocher, M., Mauser, W., Hank, T., 2017. Retrieval of biophysical crop variables from multi-angular canopy spectroscopy. Remote Sens. 9. https://doi.org/10.3390/rs9070726.

Egerer, M.H., Arel, C., Otoshi, M.D., Quistberg, R.D., Bichier, P., Philpott, S.M., 2017. Urban arthropods respond variably to changes in landscape context and spatial scale. J. Urban Econ. 3 (1), jux001. https://doi.org/10.1093/JUE/JUX001.

Ehbrecht, M., Schall, P., Ammer, C., Seidel, D., 2017. Quantifying stand structural complexity and its relationship with forest management, tree species diversity and microclimate. Agric. For. Meteorol. 242, 1–9. https://doi.org/10.1016/J.AGRFORMET.2017.04.012.

Erlandsson, R., Arneberg, M.K., Tømmervik, H., Finne, E.A., Nilsen, L., Bjerke, J.W., 2023. Feasibility of active handheld NDVI sensors for monitoring lichen ground cover. Fungal Ecol 63, 1754–5048. https://doi.org/10.1016/j.funeco.2023.101233.

Farwell, L.S., Gudex-Cross, D., Anise, I.E., Bosch, M.J., Olah, A.M., Radeloff, V.C., Razenkova, E., Rogova, N., Silveira, E.M.O., Smith, M.M., Pidgeon, A.M., 2021. Satellite image texture captures vegetation heterogeneity and explains patterns of bird richness. Remote Sens. Environ. 253, 112175. https://doi.org/10.1016/j.rse.2020.112175.

Fassnacht, F.E., Latifi, H., Nasir, K., Straub, C., Stereńczak, K., Modzelewska, A., Lefsky, M., Waser, L.T., Ghosh, A., 2016. Review of studies on tree species classification from remotely sensed data. Elsevier. In: Fassnacht, F.E., Latifi, H., Stereńczak, K., Modz, A., Lefsky, M., Waser, L.T., Straub, C. (Eds.), Remote Sens. Environ. 2016•Elsevier. https://doi.org/10.1016/j.rse.2016.08.013.

Fj Aronson, M., Lepczyk, C.A., Evans, K.L., Goddard, M.A., Lerman, S.B., Macivor, S., Nilon, C.H., Vargo, T., 2017. Biodiversity in the city: key challenges for urban green space management. Wiley Online Libr. In: Aronson, Lepczyk, C.A., Evans, K.L., Goddard, M.A., Lerman, S.B., MacIvor, J.S., Nilon, C.H. (Eds.), Frontiers Ecol. Environ. 2017•Wiley Online Libr, pp. 189–196. https://doi.org/10.1002/fee.1480, 15.

Flynn, D.F.B., Mirotchnick, N., Jain, M., Palmer, M.I., Naeem, S., 2011. Functional and phylogenetic diversity as predictors of biodiversity- ecosystem-function relationships. Ecology 92, 1573–1581. https://doi.org/10.1890/10-1245.1;PAGEGROUP:STRING:PUBLICATION.

Gadow, K.v., Zhang, C.Y., Wehenkel, C., Pommerening, A., Corral-Rivas, J., Korol, M., Myklush, S., Hui, G.Y., Kiviste, A., Zhao, X.H., 2012. Forest Structure and Diversity, pp. 29–83. https://doi.org/10.1007/978-94-007-2202-6_2.

Getzin, S., Wiegand, K., Schöning, I., 2012. Assessing biodiversity in forests using very high-resolution images and unmanned aerial vehicles. Methods Ecol. Evol. 3, 397–404. https://doi.org/10.1111/J.2041-210X.2011.00158.X;REQUESTEDJOURNAL:JOURNAL:2041210X;WEBSITE:WEBSITE:BESJOURNALS;WGROUP:STRING:PUBLICATION.

Gholizadeh, H., Gamon, J.A., Zygielbaum, A.I., Wang, R., Schweiger, A.K., Cavender-Bares, J., 2018. Remote sensing of biodiversity: soil correction and data dimension reduction methods improve assessment of α-diversity (species richness) in prairie ecosystems. Remote Sens. Environ. 206, 240–253. https://doi.org/10.1016/j.rse.2017.12.014.

Grabska, E., Frantz, D., Ostapowicz, K., 2020. Evaluation of machine learning algorithms for forest stand species mapping using Sentinel-2 imagery and environmental data in the Polish carpathians. Remote Sens. Environ. 251, 112103. https://doi.org/10.1016/J.RSE.2020.112103.

Haralick, R.M., Dinstein, I., Shanmugam, K., 1973. Textural features for image classification. IEEE Trans. Syst. Man Cybern. SMC-3, 610–621. https://doi.org/10.1109/TSMC.1973.4309314.

Hauser, L.T., Timmermans, J., van der Windt, N., Sil, Â.F., César de Sá, N., Soudzilovskaia, N.A., van Bodegom, P.M., 2021. Explaining discrepancies between spectral and in-situ plant diversity in multispectral satellite earth observation. Remote Sens. Environ. 265. https://doi.org/10.1016/j.rse.2021.112684.

Hofmann, S., Everaars, J., Schweiger, O., Frenzel, M., Bannehr, L., Cord, A.F., 2017. Modelling patterns of pollinator species richness and diversity using satellite image texture. PLoS One 12, 1–17. https://doi.org/10.1371/journal.pone.0185591.

Ishii, H.R., 2004. Exploring the relationships among canopy structure. Stand Product. Biodiv. Temp. Forest Ecosyst. https://doi.org/10.1093/forestscience/50.3.342.

Knipling, E.B., 1970. Physical and physiological basis for the reflectance of visible and near-infrared radiation from vegetation. Remote Sens. Environ. 1, 155–159. https://doi.org/10.1016/S0034-4257(70)80021-9.

Kruse, F.A., Lefkoff, A.B., Boardman, J.W., Heidebrecht, K.B., Shapiro, A.T., Barloon, P.J., Goetz, A.F.H., 1993. The spectral image processing system (SIPS)—Interactive visualization and analysis of imaging spectrometer data. Remote Sens. Environ. 44, 145–163. https://doi.org/10.1016/0034-4257(93)90013-N.

Levin, N., Shmida, A., Levanoni, O., Tamari, H., Kark, S., 2007. Predicting mountain plant richness and rarity from space using satellite-derived vegetation indices. Divers. Distrib. 13, 692–703. https://doi.org/10.1111/j.1472-4642.2007.00372.x.

Lin, B., Philpott, S., 2015. The Future of Urban Agriculture and biodiversity-ecosystem Services: Challenges and next Steps. ecology, S.J.-B. and applied, 2015, undefined. Elsevier. https://doi.org/10.1016/j.baae.2015.01.005, 16.

Lin, B.B., Egerer, M.H., Liere, H., Jha, S., Bichier, P., Philpott, S.M., 2018. Local- and landscape-scale land cover affects microclimate and water use in urban gardens. Sci. Total Environ. 610–611, 570–575. https://doi.org/10.1016/J.SCITOTENV.2017.08.091.

Luis Hernández-Stefanoni, J., Gallerdo-Cruz, J.A., Meave, J.A., Rocchini, D., Bello-Pineda, J., Omar López-Martínez, J., 2012. Modeling α-and β-diversity in a Tropical Forest from Remotely Sensed and Spatial Data. Elsevier. https://doi.org/10.1016/j.jag.2012.04.002.

Madonsela, S., Cho, M.A., Ramoelo, A., Mutanga, O., 2017. Remote sensing of species diversity using Landsat 8 spectral variables. ISPRS J. Photogrammetry Remote Sens. 133, 116–127. https://doi.org/10.1016/J.ISPRSJPRS.2017.10.008.

McElhinny, C., Gibbons, P., Brack, C., Bauhus, J., 2005. Forest and woodland stand structural complexity: its definition and measurement. For. Ecol. Manage. 218, 1–24. https://doi.org/10.1016/J.FORECO.2005.08.034.

Muro, J., Linstädter, A., Magdon, P., Wöllauer, S., Männer, F.A., Schwarz, L.M., Ghazaryan, G., Schultz, J., Malenovský, Z., Dubovyk, O., 2022. Predicting plant biomass and species richness in temperate grasslands across regions, time, and land management with remote sensing and deep learning. Remote Sens. Environ. 282, 113262. https://doi.org/10.1016/j.rse.2022.113262.

O'Brien, S.T., Hubbell, S.P., Spiro, P., Condit, R., Foster, R.B., 1995. Diameter, height, crown, and Age relationship in eight neotropical tree species. Ecology 76, 1926–1939. https://doi.org/10.2307/1940724.

Palmer, M.W., Earls, P.G., Hoagland, B.W., White, P.S., Wohlgemuth, T., 2002. Quantitative tools for perfecting species lists. Environmetrics 13, 121–137. https://doi.org/10.1002/env.516.

Picard, R.R., Cook, R.D., 1984. Cross-validation of regression models. J. Am. Stat. Assoc. 79, 575–583. https://doi.org/10.1080/01621459.1984.10478083;WGROUP:STRING:PUBLICATION.

Rocchini, D., Balkenhol, N., Carter, G.A., Foody, G.M., Gillespie, T.W., He, K.S., Kark, S., Levin, N., Lucas, K., Luoto, M., Nagendra, H., Oldeland, J., Ricotta, C., Southworth, J., Neteler, M., 2010a. Remotely sensed spectral heterogeneity as a proxy of species diversity: recent advances and open challenges. Ecol. Inform. 5, 318–329. https://doi.org/10.1016/j.ecoinf.2010.06.001.

Rocchini, D., Balkenhol, N., Carter, G.A., Foody, G.M., Gillespie, T.W., He, K.S., Kark, S., Levin, N., Lucas, K., Luoto, M., Nagendra, H., Oldeland, J., Ricotta, C., Southworth, J., Neteler, M., 2010b. Remotely sensed spectral heterogeneity as a proxy of species diversity: recent advances and open challenges. Ecol. Inform. 5, 318–329. https://doi.org/10.1016/j.ecoinf.2010.06.001.

Rocchini, D., Marcantonio, M., Ricotta, C., 2017. Measuring Rao's Q diversity index from remote sensing: an open source solution. Ecol. Indic. 72, 234–238. https://doi.org/10.1016/J.ECOLIND.2016.07.039.

Rouse, J., Haas, R., Schell, J., Publ, D.D.-N.S., 1974. Undefined, N.D. Monitoring Vegetation Systems in the Great Plains with ERTS. Books.Google. com.

Schneider, F.D., Morsdorf, F., Schmid, B., Petchey, O.L., Hueni, A., Schimel, D.S., Schaepman, M.E., 2017. Mapping functional diversity from remotely sensed morphological and physiological forest traits. Nat. Commun. 8. https://doi.org/10.1038/s41467-017-01530-3.

Shan, G., 2022. Monte carlo cross-validation for a study with binary outcome and limited sample size. BMC Med. Inf. Decis. Making 22, 1–15. https://doi.org/10.1186/S12911-022-02016-Z/FIGURES/11.

Shannon, C.E., 1948. A mathematical theory of communication. Bell Syst. Tech. J. 27, 379–423. https://doi.org/10.1002/J.1538-7305.1948.TB01338.X.

St-Louis, V., Pidgeon, A.M., Radeloff, V.C., Hawbaker, T.J., Clayton, M.K., 2006. High-resolution image texture as a predictor of bird species richness. Remote Sens. Environ. 105, 299–312. https://doi.org/10.1016/j.rse.2006.07.003.

Torresani, M., Rocchini, D., Sonnenschein, R., Zebisch, M., Hauffe, H.C., Heym, M., Pretzsch, H., Tonon, G., 2020. Height variation hypothesis: a new approach for estimating forest species diversity with CHM LiDAR data. Ecol. Indic. 117. https://doi.org/10.1016/j.ecolind.2020.106520.

Tuanmu, M.N., Jetz, W., 2015. A global, remote sensing-based characterization of terrestrial habitat heterogeneity for biodiversity and ecosystem modelling. Global Ecol. Biogeogr. 24, 1329–1339. https://doi.org/10.1111/geb.12365.

Turner, W., Spector, S., Gardiner, N., Fladeland, M., Sterling, E., Steininger, M., 2003. Remote sensing for biodiversity science and conservation. Trends Ecol. Evol. 18, 306–314. https://doi.org/10.1016/S0169-5347(03)00070-3.

Van Cleemput, E., Adler, P., Suding, K.N., 2023. Making remote sense of biodiversity: what grassland characteristics make spectral diversity a good proxy for taxonomic diversity? Global Ecol. Biogeogr. 32, 2177–2188. https://doi.org/10.1111/geb.13759.

Vihervaara, P., Auvinen, A.P., Mononen, L., Törmä, M., Ahlroth, P., Anttila, S., Böttcher, K., Forsius, M., Heino, J., Heliölä, J., Koskelainen, M., Kuussaari, M., Meissner, K., Ojala, O., Tuominen, S., Viitasalo, M., Virkkala, R., 2017. How essential biodiversity variables and remote sensing can help national biodiversity monitoring. Glob. Ecol. Conserv. 10, 43–59. https://doi.org/10.1016/J.GECCO.2017.01.007.

Wagner, B., Egerer, M., 2022. Application of UAV remote sensing and machine learning to model and map land use in urban gardens. J. Urban Econ. 8, 1–12. https://doi.org/10.1093/jue/juac008.

Wang, R., Gamon, J.A., 2019. Remote sensing of terrestrial plant biodiversity. Remote Sens. Environ. 231, 111218. https://doi.org/10.1016/j.rse.2019.111218.

Wang, R., Gamon, J.A., Cavender-Bares, J., Townsend, P.A., Zygielbaum, A.I., 2018. The spatial sensitivity of the spectral diversity–biodiversity relationship: an experimental test in a prairie grassland. Ecol. Appl. 28, 541–556. https://doi.org/10.1002/EAP.1669.

Wang, R., Gamon, J.A., Emmerton, C.A., Li, H., Nestola, E., Pastorello, G.Z., Menzer, O., 2016. Integrated analysis of productivity and biodiversity in a southern Alberta prairie. Remote Sens. 8, 1–20. https://doi.org/10.3390/rs8030214.

Wang, S., Loreau, M., 2016. Biodiversity and ecosystem stability across scales in metacommunities. Ecol. Lett. 19, 510–518. https://doi.org/10.1111/ELE.12582.

White, J.C., Gómez, C., Wulder, M.A., Coops, N.C., 2010. Characterizing temperate forest structural and spectral diversity with hyperion EO-1 data. Remote Sens. Environ. 114, 1576–1589. https://doi.org/10.1016/j.rse.2010.02.012.

Zeng, L., Wardlow, B.D., Xiang, D., Hu, S., Li, D., Zeng, L., Wardlow, B.D., Xiang, D., Hu, L., 2020. A review of vegetation phenological metrics extraction using time-series, multispectral satellite data. Elsevier 237. https://doi.org/10.1016/j.rse.2019.111511.

Zhang, F., Yang, X., 2020. Improving land cover classification in an urbanized coastal area by random forests: the role of variable selection. Remote Sens. Environ. 251, 112105. https://doi.org/10.1016/J.RSE.2020.112105.

Zhu, X., Luleva, M., Paolini van Helfteren, S., Gou, Y., Gajda, W., Neinavaz, E., 2024a. Comparison of functional and structural biodiversity using Sentinel-2 and airborne LiDAR data in agroforestry systems. Remote Sens. Appl. Soc. Environ. 35. https://doi.org/10.1016/j.rsase.2024.101252.

Zhu, X., Luleva, M., Paolini van Helfteren, S., Gou, Y., Gajda, W., Neinavaz, E., 2024b. Comparison of functional and structural biodiversity using Sentinel-2 and airborne LiDAR data in agroforestry systems. Remote Sens. Appl. Soc. Environ. 35. https://doi.org/10.1016/j.rsase.2024.101252.